Relationships between Molecular Structure and Optical, Dielectric, and Thermal Properties of Novel Semi-alicyclic Polyimides Containing Bio-derived Isohexides

Ririka SAWADA,[a] Mitsutaka OZAKI,[b] Kazuhisa YAJIMA,[b] and Shinji ANDO [a]

[a] *Dept. Chemistry and Materials Science, Tokyo Institute of Technology, Ookayama 2-12-1-E4-5, Meguro-ku, Tokyo 152-8552, Japan*
E-mail: sawada.r.ae@m.titech.ac.jp
[b] *Honshu Chemical Industry Co. Ltd., Kozaika 2-5-115, Wakayama 641-0007, Japan*

A series of novel plant-derived polyimides (PIs) were prepared from newly synthesized dianhydrides of isosorbide (ISS)- and isomannide (ISM)-3,6-diyl-bis(trimellitic anhydride)s (ISSDA and ISMDA). The PIs from ISSDA (ISS-PIs) and those from both ISSDA and ISMDA (CoPIs) exhibited excellent optical transparency, low refractive indices (n_{av}), and small birefringence (Δn) compared to wholly aromatic PIs. This is because the in-plane orientation of the main chain and the dense molecular packing between PI chains were suppressed by the bulky alicyclic ISS structure and the bent and flexible main chains with reduced intermolecular interactions. The ISS-PIs also demonstrated lower dielectric constants (D_k) with moderate dissipation factors (D_f) at 10 and 20 GHz. Furthermore, ISS-PIs demonstrated well-defined circular dichroism (CD) in the UV region in the solid state because of the inherent optical activity of the biobased ISS, which indicates that chiral structures were maintained even in the solid PI films. In addition, the ISS-PIs had sufficient thermal stability with a glass transition temperature (T_g) of approximately 260 °C and the 5 wt % weight-loss temperatures (T_d^5) of approximately 400 °C. The ISM-containing CoPIs exhibited enhanced optical properties than ISS-TFDB (HomoPI) due to a boat-like and sterically constrained structure of ISMDA, which is supported by the systematic conformational analysis using density functional theory (DFT) calculations. The ISMDA moiety also improves the dielectric properties with lowering the D_k and D_f at 10–20 GHz due to the reduced dipolar polarization and suppression of local molecular motion. This study clarifies the mechanism underlying the enhancement of various properties induced by the incorporation of specific structures of ISS and ISM.

1. Introduction

In recent years, the use of biomass-based chemical resources has attracted considerable attention from a viewpoint of reducing the environmental load and enhancing sustainability. Cellulose, a renewable and inedible biomass obtained from plants is attractive for application in bio-based polymers because it does not compete with human food and animal feed. 1,4;3,6-Dianhydrohexitols (isohexides), which are diols derived from biomass cellulose, have bulky and rigid structures consisting of two tetrahydrofuran rings connected by a *V*-shaped linkage at 120°.[1] These include three stereoisomers (isosorbide (ISS), isomannide (ISM), and isoidide (ISI)) that are discriminated according to the directions of the two hydroxy (–OH) groups. ISS can be directly synthesized from *D*-glucose. The ability for mass production has led to extensive research on the application of ISS in commonly used plastics, such as polycarbonate (PC) and polyester (PE), with higher optical transparency and a lower refractive index than conventional plastics. In contrast, industrial applications of ISM and ISI have been difficult and limited due to their complicated synthesis,[1,2] although ISM and ISI have two *endo* or two *exo* –OH groups, respectively.

Polyimides (PIs) are high-performance polymers that exhibit excellent thermal and chemical stability, electrical insulation, and mechanical strength. Because of these excellent physical properties, PIs play an important role in microelectronics and aerospace industries. For instance, PIs have been applied in flexible printed circuit boards, interlayer dielectrics with thermal insulation, and solar sails.[3] In particular, PIs are expected to be used as dielectrics for the next-generation (5G and 6G) wireless communication at high frequencies in the GHz–THz range.[4,5] For these applications, it is desirable to achieve a low dielectric constant (D_k) between 2.8–3.2, a dissipation factor (D_f) lower than 10^{-2}, sufficient thermal stability, and mechanical strength as well as high optical transparency and low refractive index. However, application of PIs in optoelectronics is limited because of the strong coloration of PIs derived from inter- and intramolecular

charge-transfer (CT) interactions and the high dielectric constants and water absorption ability due to the polar imide group.[6,7]

In fact, although some PIs containing ISS or ISM skeletons in the main chain have been reported,[8–12] the physical properties of ISM-containing polymers have not been investigated in detail because of its complicated synthesis and low reactivity. In this study, a series of novel semi-alicyclic PIs incorporating ISS (ISS-PIs) and copolyimides containing both ISS and ISM (CoPIs) were synthesized using ISS- and ISM-derived dianhydrides (ISSDA and ISMDA) and various diamines (**Fig. 1, 2**). Their optical, dielectric, and thermal properties were analyzed for discussing their structure-property relationships and the effect of the introduction of the ISS and ISM moiety.

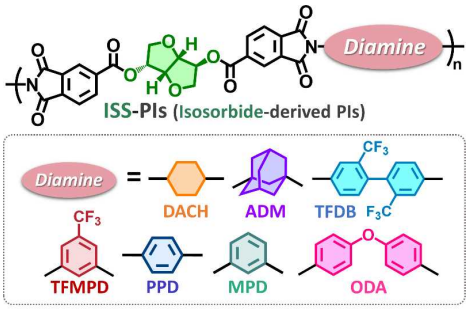

Fig. 1 Chemical structures of ISS-PIs.

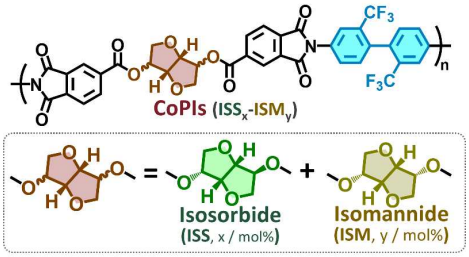

Fig. 2 Chemical structures of CoPIs.

2. Experimental

2.1 Preparation of PI films

Poly(amic acid)s (PAAs), precursors of ISS-PIs, were synthesized by ISSDA and diamines in *N,N*-dimethylacetamide (DMAc). To obtain copolymerized PAA, ISMDA and ISSDA were added stepwise into a DMAc solution of a diamine (TFDB), as a mole fraction of ISSDA : ISMDA = *x* : *y*. PAAs spin-coated on Si or silica substrates were thermally imidized at 280 °C, and then ISS-PI and CoPI films were prepared.

2.2 Measurements

The UV-visible (UV-vis) optical absorption spectra and UV-vis circular dichroism (CD) spectroscopy was acquired for the PI films formed on the fused silica substrates. CD spectroscopy was conducted in the wavelength range of 190–500 nm. In the measurements described below, the PI films formed on silicon wafers was used. The in-plane (n_{TE}) and out-of-plane (n_{TM}) refractive indices were measured by the prism coupling method at wavelengths of λ = 636, 845, 1310, and 1558 nm and the average refractive index (n_{av}) and in-plane/out-of-plane birefringence (Δn) were estimated. The dielectric constant (D_k) and dissipation factor (D_f) were measured in the transverse electric (TE) mode at 10 or 20 GHz. To avoid the influence of the measurement environment, the resonator was stored in a home-built chamber made of acrylic resin, in which the temperature and relative humidity (RH) were controlled at 23 °C and 30%RH, respectively. The T_g was evaluated from the inflection points of the thermomechanical analysis (TMA) curves and the 5 wt% weight loss temperature (T^5_d) was evaluated from thermogravimetric analysis (TGA).

3. Results and Discussion

3.1 Isosorbide-derived PIs (ISS-PIs)

The wavelength dispersions of n_{av} and Δn for ISS-PIs are plotted in **Fig. 3**. All the n_{av} and Δn values measured at 1310 nm are smaller than 1.603 and 0.021, respectively, which indicates that the ISS-PI films have lower n_{av} and smaller Δn than conventional wholly aromatic PIs such as PMDA-ODA and sBPDA-PPD (n_{av} = 1.652, 1.715, and Δn = 0.0759, 0.1700 at 1320 nm, respectively).[13,14] **Fig. 4** compares the molecular structures of ISS-ODA and PMDA-ODA with common 4,4'-ODA moieties as an example. The repeating unit of ISS-ODA has a bulkier and more bent structure than PMDA-ODA, which supports that the introduction of ISS into PIs increases the interchain free volume due to its bulky fused-ring structure. This suppresses intermolecular interaction-assisted PI chain aggregation and lowers the polarizability per unit volume (α_{av}/V_{vdw}), leading to lower refractive indices, as followed to Lorentz-Lorenz equation: $(n_{av}^2-1)/(n_{av}^2+2) = (4\pi/3)\cdot(\alpha_{av}/V_{vdw})$.[14] In addition, the locally bent structure introduced by ISSDA, while maintaining the rigid alicyclic

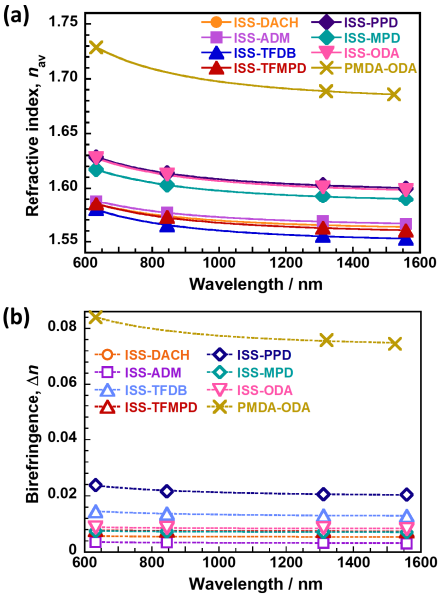

Fig. 3 Wavelength dispersions of (a) average refractive indices (n_{av}) and (b) birefringence (Δn) of ISS-PIs.

structure of ISS, suppresses the linear elongation and in-plane orientation of the PI chains, resulting in a nearly isotropic orientation with a small birefringence.

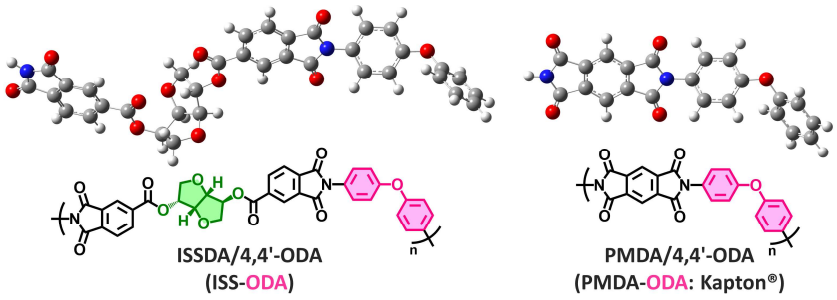

Fig. 4 Structural differences between ISS-ODA and PMDA-ODA.

In **Fig. 5**, all the D_k values are smaller than 3.33 at 10 GHz, and the fluorinated PIs, ISS-TFDB and ISS-TFMPD, show relatively smaller D_k. As discussed above, the bulky and bent backbone of ISS can effectively increase the interchain free volume and suppress tight molecular packing of the ISS-PI chains, resulting in the reduction of the α_{av}/V_{vdw}. In addition, **Fig. 5** shows that both D_k and D_f linearly increase with the content of polar imide group per unit.[15] Here, the dielectric polarization contains the contribution of the following three types of polarization: electronic (P_e), atomic (P_a), and dipolar (P_d) polarizations.[4] The reduced number of polar imide rings in the ISS-PIs per unit volume suppresses not only the P_e but also P_d, leading to low dielectric constants and losses. ISS-TFMPD, PPD, and MPD, consisting of one benzene ring in the diamine moiety, exhibited larger D_k and D_f values, whereas ISS-TFDB and ISS-ODA, which consist of two benzene rings, exhibited relatively small values. Furthermore, ISS-TFDB exhibited the lowest D_k and D_f, suggesting that the introduction of trifluoromethyl ($-CF_3$) group effectively lowered these values. Furthermore, the D_f values at 20 GHz are consistently larger than those at 10 GHz, which is partly attributable to the induction of orientational relaxation by the polar imide and ester groups, in the THz region, as well as the dynamic relaxation of water molecules absorbed or adsorbed on the PI films. As has been reported,[16] absorbed water significantly increases the D_f of PI films because the D_f of pure water molecules shows a maximum at around 20 GHz at 20–30 °C.

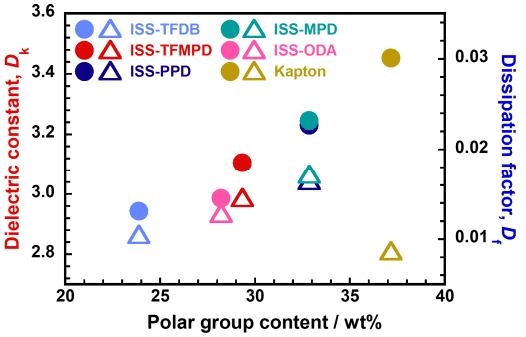

Fig. 5 Dielectric constants (D_k) and dissipation factors (D_f) of ISS-PIs at 10 GHz.

The UV–vis absorption spectra and photographs under white light of the ISS-PI thin films are shown in **Fig. 6**. The films are transparent and either totally colorless or pale yellow, which is supported by the fact that the wavelengths of the absorption edge (λ_E) are shorter than 450 nm. These are much lighter in color than those of conventional PIs; PMDA-ODA is dark yellowish brown with λ_E around 550 nm,[17] and even PMDA-TFDB containing plural fluorine atoms shows λ_E around 500 nm.[6] The optical absorption of PIs in the visible region is mainly governed by inter- and intramolecular CT interactions.[6,17] The excellent optical transparency of ISS-PIs originates from the suppression of intermolecular CT interactions by the bulky and bent structure of ISS in the dianhydride moiety (**Fig. 4**).[18] As shown in **Fig. 6**, the λ_E of ISS-DACH and ISS-ADM appear at the shortest wavelengths because of the suppression of CT interactions originating from the alicyclic diamine structures. Besides, the λ_Es of ISS-TFMPD and ISS-MPD are in the UV region, indicating that the PIs derived from aromatic diamines with *meta*-phenylene linkages exhibit sufficiently high optical transparency, and ISS-TFMPD showed the

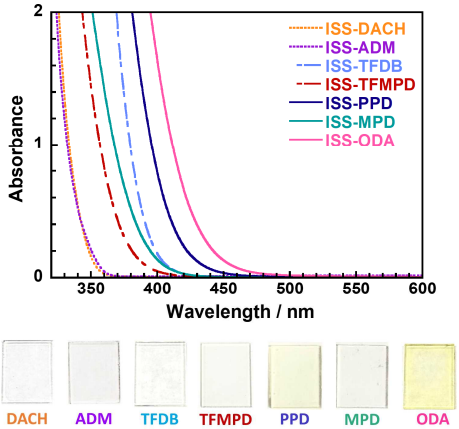

Fig. 6 UV-vis absorption spectra and appearance of ISS-PIs.

highest optical transparency among the aromatic ISS-PIs, owing to the combination of *meta*-phenylene and $-CF_3$ side groups. Note that the transparency of ISS-TFMPD is superior to that of ISS-TFDB, indicating that the bent backbone structure is more effective at improving transparency than the $-CF_3$ content. In contrast, the λ_Es of ISS-ODA and ISS-PPD are located in the visible region at approximately 450 nm due to the enhanced CT interactions that stem from the strong electron-donating properties of ODA and PPD, resulting in pale-yellow films.[6]

The UV–vis CD spectra of solid ISS-PI films are shown in **Fig. 7**. Each ISS-PI CD spectrum exhibits split signals consisting of a negative peak at 230–238 nm and a positive peak at 208–214 nm, same as that of the low-molecular-weight model compounds of cyclohexyl-capped ISSDA (ISS-2Ch). Note that the CD spectra of ISS-DACH and ISS-ADM with alicyclic diamines show sharply split signals centered at approximately 225 nm originated from the exciton coupling between trimellitic (TME) group,[19] which are quite similar to those of ISS-2Ch. Similarly, the aromatic ISS-PIs showed a split signal centered at approximately 225 nm. On the basis of the theory of exciton chirality,[19–21] these indicate that a negative chirality caused by exciton interactions, which was observed for all ISS-PIs as well as ISS-2Ch. Note that the twisted counter-clockwise configuration between the TME groups is well maintained in the solid ISS-PI thin films, which is attributable to the restricted conformational changes around the ISS moiety.

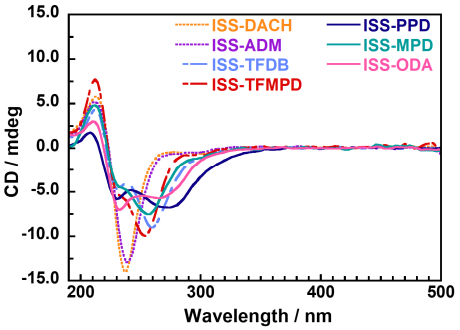

Fig. 7 CD spectra of solid ISS-PI films.

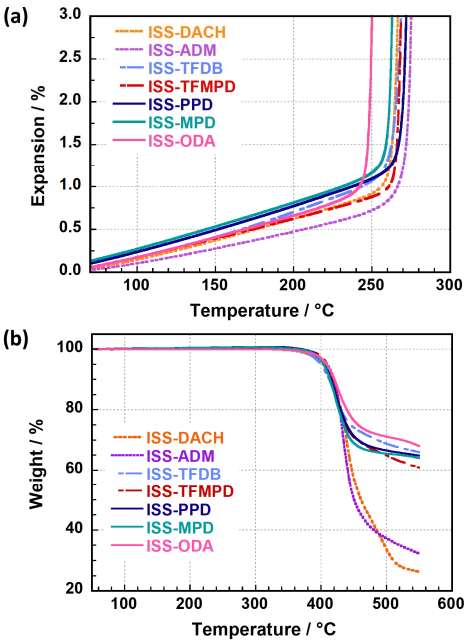

Fig. 8 (a) TMA and (b) TGA curves of ISS-PIs.

The TMA and TGA curves of the ISS-PIs are shown in **Fig. 8**. All the samples demonstrate T_g and T_d^5 values higher than 240 °C and 400 °C, and the average values are 260 and 406 °C, respectively, indicating that the ISS-PIs have sufficient thermal stability for optoelectronic and dielectric applications. The lowest T_g of ISS-ODA (240 °C) is attributable to the rotatable ether linkage, whereas ISS-TFMPD, PPD, and MPD, having only one benzene ring in their diamine moieties, exhibited higher T_gs. ISS-PPD exhibited the highest T_g of 268 °C owing to the restrained segmental motion of the PI chain. It is interesting that the T_g of ISS-TFMPD (265 °C) with a *meta*-phenylene linkage was slightly higher than that of ISS-TFDB (258 °C) with a linear biphenyl structure. Note that the rotational motion of the two N(imide)–C(phenyl) bonds attached to the *meta*-phenylene of ISS-TFMPD should be much more restricted in the solid state than that of ISS-TFDB. The latter can undergo both π–flip rotational motion at the *para*-linked biphenyl-imide structures and fluctuation of the polymer backbone, whereas the former undergoes only fluctuation of the polymer backbone.[22]

3.2 Isomannide-incorporating ISS-PIs (CoPIs)

The specific characteristics of the stem of the ISM skeleton were determined by analyzing the two *endo*–OH groups bonded to the fused aliphatic ring. Conformational energy analysis was conducted by varying the two dihedral angles at both ester C–O bonds (φ and ψ) of the model compounds of the isohexide-derived ester imides (ISM-DI and ISS-DI) at intervals of 15°. The molecular geometry was optimized at each conformation with fixed values of φ and ψ. The calculated conformational energy surfaces of the ester imide model compounds are presented in **Fig. 9**. Notably, the energetically allowed conformations for ISM-DI (*e.g.,* <5 kJ mol^{-1} ≈ 2*RT* at 300 K) are significantly limited to a small area around (φ, ψ) = (170°, 170°), which corresponds to a boat-shaped bent structure, as shown in **Fig. 9(a)**. In contrast, the energetically allowed conformations of ISS-DI is broadly distributed over the energy surfaces (**Fig. 9(b)**), as these imides have flexible structures with more rotational freedom. These calculated results strongly support the appreciable steric hindrance and the high rotational barriers around the ISM moiety.[12]

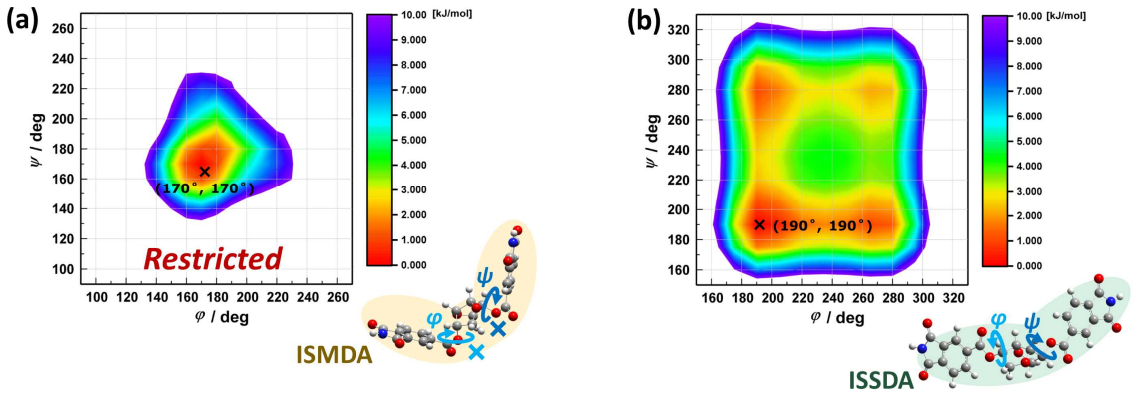

Fig. 9 Conformational energy surfaces of (a) ISM-DI and (b) ISS-DI as model compounds.

The wavelength dispersions of n_{av} and Δn for CoPIs and HomoPI (ISS-TFDB) are displayed in **Fig. 10**. The n_{av} of the CoPIs was similar to that of HomoPI (n_{av} = 1.557 at 1310 nm), and significantly lower than that of a PI derived from PMDA and TFDB (n_{av} = 1.573).[14] As shown above, the ISM-containing repeating unit has a boat-like bent structure, whereas the only ISS-containing repeating unit has a relatively elongated structure, indicating that a small amount of ISMDA skeleton incorporated in the CoPI chains may reduce the main chain orientation and then the α_{av}/V_{vdw}. Note that the smallest n_{av} was observed for ISS_7–ISM_3, which indicates that the structural specificity of ISMDA has the most significant effect in the case of the molar content of ISMDA in CoPIs (C_m) is equal to 30. As shown in **Fig. 10(b)**, the largest Δn value of HomoPI (Δn = 0.0130) monotonically decreased with an increase in C_m (0.0093 < Δn < 0.0121), indicating that the macroscopic polarizability anisotropy is reduced due to the conformational disorder in the CoPI chains caused by the ISMDA moiety. The relatively large Δn of HomoPI is due to the structural linearity and the preferential in-plane orientation of the main chains, whereas the bent and boat-shaped ISMDA moiety brings disorder to the ISS–TFDB segment in the CoPIs. Furthermore, the Δn values for the CoPIs with C_m > 40 are very small, even though the n_{av} values are comparable to those of ISS_7–ISM_3, which is due to the inherently smaller polarizability anisotropy of the ISM–TFDB repeating unit. In any case, the values of Δn are much smaller than that of PMDA–TFDB (Δn = 0.1232) [14] and other semi-alicyclic PIs derived from ISS and PPD (Δn = 0.02),[23] as well as homo ISS–TFDB.

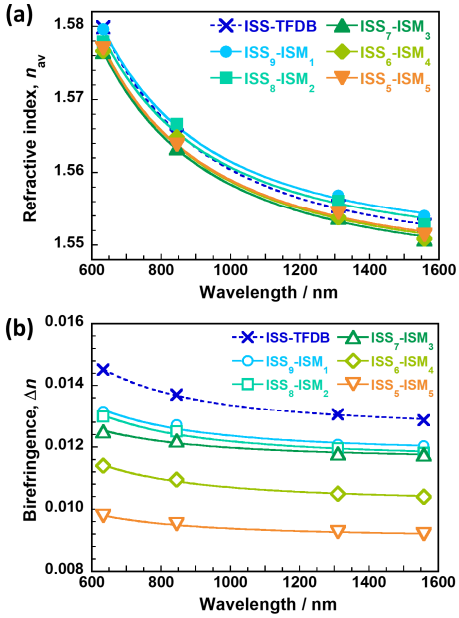

Fig. 10 Wavelength dispersions of (a) n_{av} and (b)Δn of CoPIs.

Fig. 11 summarizes the D_k and D_f for the CoPIs measured at 10 GHz. The D_k values of the CoPIs with 10 ≤ C_m ≤ 30 are smaller than that of HomoPI (D_k < 2.97), indicating that the incorporation of a certain amount of ISM effectively decreases D_k, and the D_k exhibits a minimum value at C_m = 30 (D_k = 2.92). As discussed above, the n_{av} values of CoPIs become smaller with an increase in C_m from 10 to 30, whereas the D_k remained nearly constant with a further addition of ISM. It is important to note that ISS_7–ISM_3 exhibits the smallest D_k as well as smallest n_{av} at 1310 nm. This also implies that the D_k of the CoPIs is closely related to the n_{av} values, as evidenced by Maxwell's formula. The D_f values of the CoPIs with C_m ≤ 30 are smaller than that of HomoPI. In particular, the incorporation of only 10 mol% of ISM considerably lowers the D_f, which indicates that the molecular motion out of sync with 10–20 GHz is effectively suppressed by the high rotational barrier at both ends of the

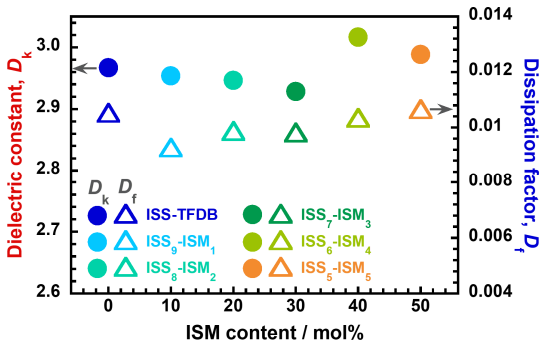

Fig. 11 D_k and D_f of CoPI at 10 GHz.

ISM moiety. In contrast, the D_f values of the CoPIs with $C_m > 30$ are larger than those of HomoPI and the other CoPIs, resulting in a monotonic increase in D_f with an increase in C_m.

Fig. 12(a) shows the UV-vis absorption spectra of HomoPI and CoPI films thermally imidized at 220 °C and the photographs taken under white light. All the CoPI films were colorless and transparent without any absorption in the visible region, resulting in superior optical transparency in contrast to the conventional PIs such as PMDA-ODA and even to the ISS-PIs. This originates from the significant reduction of the intermolecular CT interactions due to the bent ISMDA skeleton.[6,23] Remarkably, the optical transparency was improved by adding only C_m = 10, indicating the effectiveness of the ISM structure. Note that the CoPI films show a lighter color, and the λ_E of the CoPIs are shorter than that of HomoPI, even when the films were thermally imidized at 320 °C, as shown in **Fig. 12(b)**. The λ_E of the HomoPI imidized at 320 °C, which has a light brown color, is shifted to a longer wavelength (λ_E < 500 nm) than that imidized at 220 °C. The vigorous molecular motion occurring over its T_g (= 258 °C) may promote partial aggregation of ISS–TFDB units after cooling. In contrast, the films of CoPIs except for ISS_6–ISM_4 and ISS_5–ISM_5 thermally imidized at 320 °C are colorless and transparent because their reduced intermolecular CT interactions were kept even after the high-temperature treatment.

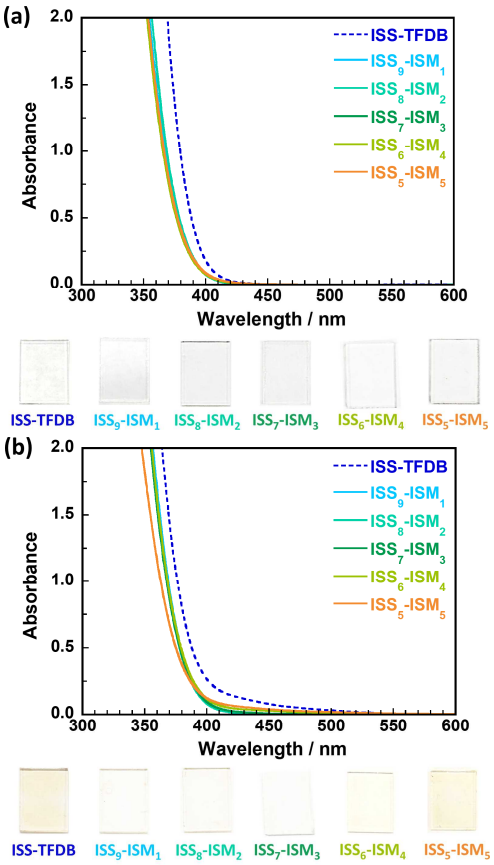

Fig. 12 UV-vis absorption spectra and appearance of CoPIs imidized at (a) 220 °C and (b) 320 °C.

Fig. 13 shows the TMA and TGA curves of the CoPIs. All CoPIs exhibit T_gs higher than 256 °C, which suffices the general requirements of colorless and transparent PIs. It has been reported that the PIs incorporating the ISM moiety exhibited higher T_gs than that with ISS because the *exo–exo* oriented boat structure of ISM is more rigid than that of the *endo–exo* oriented chair structure of ISS.[12,24] Accordingly, the slightly higher T_g of ISS_7–ISM_3 may be attributable to the suppression of the main chain motion involved in the glass transition due to the sterically hindered ISM backbone. It has been reported that the first thermal decomposition of the isohexide skeleton is attributed to the oxidation of α-carbons occurring below 450 °C.[25] Although no significant difference was observed for the T_d^5s of CoPIs, it is interesting to note that the CoPIs exhibited higher T_d^5 than HomoPI, which suggests that the ISM moiety offers a slightly higher decomposition temperature than ISS due to the difference in configuration.

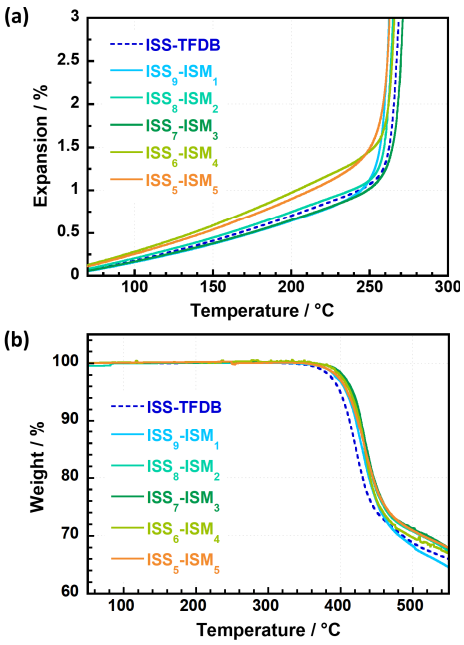

Fig. 13 (a) TMA and (b) TGA curves of CoPIs.

4. Conclusion

In summary, a series of novel alicyclic ISS-PIs and CoPIs incorporating ISS and ISM moieties were synthesized from the biobased dianhydrides (ISSDA and ISMDA) and a fluorinated TFDB diamine. ISS-PIs, derived from ISSDA and some kinds of diamines, exhibit a low refractive index (n_{av} < 1.603), low birefringence (Δn < 0.02), excellent optical transparency in the visible region, and low dielectric constant (2.97 < D_k < 3.33 at 10 GHz), compared with existing aromatic and semi-aliphatic PIs. In particular, the ISS-PI films with cyclohexyl rings, *m*-phenylene moieties, and fluorine groups exhibit colorless transparent thin films and extremely low n_{av} and Δn due to suppression of the aggregation-induced CT interactions

inhibited by the bulky and bent main-chain structures. The ISS-PI thin films show clear circular dichroism in the UV region due to the inherent optical activity of the ISS backbone, and the trimellitic groups at both ends of ISS are assumed to be fixed in a counter-clockwise conformation in the thin film state. Furthermore, ISS-PIs exhibits sufficient thermal stability (T_g > 240 °C, T_d^5 > 400 °C), confirming the well-balanced properties. However, the dissipation factors corresponding to the dielectric losses by the local molecular motion, are relatively large (D_f > 0.01) due to the high flexibility and molecular mobility.

CoPIs incorporating ISM moiety with specific conformations exhibit enhanced optical, dielectric, and thermal properties than those of HomoPIs. Based on the DFT calculations, the energetically allowed conformations of ISM-DI are limited in a significantly small area, which corresponds to a boat-shaped and sterically constrained structure, whereas those of ISS-DI are widely distributed over the energy surfaces due to the greater rotational freedom of the flexible structures. Compared with conventional entirely aromatic PIs and ISS-PIs, the CoPI films exhibited excellent optical transparency in the visible region, comparable or lower refractive indices (1.554 < n_{av} < 1.557), lower dielectric constants (2.92 < D_k < 3.02 at 10 GHz), and smaller birefringence (0.009 < Δn < 0.012). These results are attributable to the bulky and boat-like bent structure of ISMDA, which endows low polarizability and anisotropy to the repeating unit, as estimated by DFT calculations. Notably, the CoPI with only C_m = 10 demonstrated the lowest dissipation factor (D_f = 0.00928 at 10 GHz), indicating that the ISM moiety exerts an inhibitory effect on the local molecular motion of the main chain. For the series of ISS- and ISM-PIs derived from TFDB, the CoPIs with C_m = 30 exhibited the highest thermal stability, with T_g = 265 °C and T_d^5 = 417 °C. This study proposes a novel dianhydride, ISMDA, which can be readily copolymerized with ISSDA to afford improved optical, dielectric, and thermal properties owing to the reduction in the main chain orientation and conformational anisotropy and the suppression of molecular motion by the rigid and bent structure. The structure-property relationships of the isohexides-containing PIs clarified in this study can contribute to technological development and to expanding the usage of the ISM as well as ISS in bio-based polymers.

References

[1] F. Fenouillot, A. Rousseau, G. Colomines, R. Saint-Loup, J.P. Pascault, **Polymers from renewable 1,4:3,6-dianhydrohexitols (isosorbide, isomannide and isoidide): A review**, *Prog. Polym. Sci.* 35 (2010) 578–622. https://doi.org/10.1016/j.progpolymsci.2009.10.001.

[2] C. Dussenne, T. Delaunay, V. Wiatz, H. Wyart, I. Suisse, M. Sauthier, **Synthesis of isosorbide: An overview of challenging reactions**, *Green Chem.* 19 (2017) 5332–5344. https://doi.org/10.1039/c7gc01912b.

[3] G. Rabilloud, High-Performance Polymers: Polyimides in Electronics, Editions Technip, 2000.

[4] J.O. Simpson, A.K. St.Clair, **Fundamental insight on developing low dielectric constant polyimides**, *Thin Solid Films*. 308–309 (1997) 480–485. https://doi.org/10.1016/S0040-6090(97)00481-1.

[5] G. Maier, **Low dielectric constant polymers for microelectronics**, *Prog. Polym. Sci.* 26 (2001) 3–65. https://doi.org/10.1016/S0079-6700(00)00043-5.

[6] S. Ando, T. Matsuura, S. Sasaki, **Coloration of aromatic polyimides and electronic properties of their source materials**, *Polym. J.* 29 (1997) 69–76. https://doi.org/10.1295/polymj.29.69.

[7] M. Hasegawa, K. Horie, **Photophysics, photochemistry, and optical properties of polyimides**, *Prog. Polym. Sci.* 26 (2001) 259–335. https://doi.org/10.1016/S0079-6700(00)00042-3.

[8] H. Ren, Y. Guan, Y. He, H. He, X. Wang, **Polyimide Containing Isosorbide Units: Synthesis and Characterization**, *Acta Polym. Sin.* 006 (2006) 248–252. https://doi.org/10.3724/SP.J.1105.2006.00248.

[9] X. Ji, Z. Wang, J. Yan, Z. Wang, **Partially bio-based polyimides from isohexide-derived diamines**, *Polymer (Guildf).* 74 (2015) 38–45. https://doi.org/10.1016/j.polymer.2015.07.051.

[10] C.K. Chen, Y.C. Lin, L.C. Hsu, J.C. Ho, M. Ueda, W.C. Chen, **High Performance Biomass-Based Polyimides for Flexible Electronic Applications**, *ACS Sustain. Chem. Eng.* 9 (2021) 3278–3288. https://doi.org/10.1021/acssuschemeng.0c08959.

[11] G. Yang, R. Zhang, H. Huang, L. Liu, L. Wang, Y. Chen, **Synthesis of novel biobased polyimides derived from isomannide with good optical transparency, solubility and thermal stability**, *RSC Adv.* 5 (2015) 67574–67582. https://doi.org/10.1039/C5RA14526K.

[12] Z. Mi, Z. Liu, J. Yao, C. Wang, C. Zhou, D. Wang, X. Zhao, H. Zhou, Y. Zhang, C. Chen, **Transparent and soluble polyimide films from 1,4:3,6-dianhydro-D-mannitol based dianhydride and diamines containing aromatic and semiaromatic units: Preparation, characterization, thermal and mechanical properties**, *Polym. Degrad. Stab.* 151 (2018) 80–89. https://doi.org/10.1016/j.polymdegradstab.2018.01.006.

[13] S. Ando, Y. Watanabe, T. Matsuura, **Wavelength dependence of refractive indices of polyimides in visible and near-IR regions**, *Japanese J. Appl. Physics, Part 1 Regul. Pap. Short Notes Rev. Pap.* 41 (2002) 5254–5258. https://doi.org/10.1143/JJAP.41.5254.

[14] Y. Terui, S. Ando, **Coefficients of molecular packing and intrinsic birefringence of aromatic polyimides estimated using refractive indices and molecular polarizabilities**, *J. Polym. Sci. Part B Polym. Phys.* 42 (2004) 2354–2366. https://doi.org/10.1002/polb.20114.

[15] C.-C.C. Kuo, Y.-C.C. Lin, Y.-C.C. Chen, P.-H.H. Wu, S. Ando, M. Ueda, W.-C.C. Chen, **Correlating the Molecular Structure of Polyimides with the Dielectric Constant and Dissipation Factor at a High Frequency of 10 GHz**, *ACS Appl. Polym. Mater.* 3 (2021) 362–371. https://doi.org/10.1021/acsapm.0c01141.

[16] W.J. Ellison, **Permittivity of pure water, at standard atmospheric pressure, over the frequency range 0-25 THz and the temperature range 0-100 °C**, *J. Phys. Chem. Ref. Data*. 36 (2007) 1–18. https://doi.org/10.1063/1.2360986.

[17] J. Wakita, H. Sekino, K. Sakai, Y. Urano, S. Ando, **Molecular design, synthesis, and properties of highly fluorescent polyimides**, *J. Phys. Chem. B*. 113 (2009) 15212–15224. https://doi.org/10.1021/jp9072922.

[18] C. Bas, C. Tamagna, T. Pascal, N. Dominique Alberola, **On the Dynamic Mechanical Behavior of Polyimides Based on Aromatic and Alicyclic Dianhydrides**, *Polym. Eng. Sci.* 43 (2003) 344–355. https://doi.org/10.1002/pen.10029.

[19] N. Berova, L. Di Bari, G. Pescitelli, **Application of electronic circular dichroism in configurational and conformational analysis of organic compounds**, *Chem. Soc. Rev.* 36 (2007) 914–931. https://doi.org/10.1039/b515476f.

[20] R. Carr, R. Puckrin, B.K. McMahon, R. Pal, D. Parker, L.O. Pålsson, **Induced circularly polarized luminescence arising from anion or protein binding to racemic emissive lanthanide complexes**, *Methods Appl. Fluoresc.* 2 (2014). https://doi.org/10.1088/2050-6120/2/2/024007.

[21] N. Harada, **The enduring legacy of Koji Nakanishi's research on natural products and bioorganic chemistry. Part 2. Inception and establishment of the ECD exciton chirality method in 1960s to 1970s: A marvel of Nakanishi's Japanese team**, *Chirality*. 32 (2020) 535–546. https://doi.org/10.1002/chir.23193.

[22] T. Okada, R. Ishige, S. Ando, **Effects of chain packing and structural isomerism on the anisotropic linear and volumetric thermal expansion behaviors of polyimide films**, *Polymer (Guildf).* 146 (2018) 386–395. https://doi.org/10.1016/j.polymer.2018.05.059.

[23] R. Sawada, S. Ando, **Colorless, Low Dielectric, and Optically Active Semialicyclic Polyimides Incorporating a Biobased Isosorbide Moiety in the Main Chain**, *Macromolecules*. 55 (2022) 6787–6800. https://doi.org/10.1021/acs.macromol.2c01288.

[24] X. Ji, Z. Wang, Z. Wang, J. Yan, **Bio-based poly(ether imide)s from isohexide-derived isomeric dianhydrides**, *Polymers (Basel).* 9 (2017) 569. https://doi.org/10.3390/polym9110569.

[25] L. Jasinska, M. Villani, J. Wu, D. Van Es, E. Klop, S. Rastogi, C.E. Koning, **Novel, fully biobased semicrystalline polyamides**, *Macromolecules*. 44 (2011) 3458–3466. https://doi.org/10.1021/ma200256v.